Fermilab Library
0 1160 0032059 2

FERMILAB
MAY 12 1994
LIBRARY

STEWARD-1191

PREPRINTS

of the

STEWARD OBSERVATORY

THE UNIVERSITY OF ARIZONA
TUCSON, ARIZONA 85721 U.S.A.

No. 1191

THE IONIZED ISM IN LOCAL GROUP GALAXIES

Robert C. Kennicutt, Jr.

Steward Observatory
University of Arizona

Review to appear in
"The Local Group: Comparative and Global Properties",
The Third ESO/CTIO Workshop,
La Serena, January 1994,
ed. J. Storm, A. Layden, C. Smith,
ESO Conference Proceedings Series

THE IONIZED ISM IN LOCAL GROUP GALAXIES

Robert C. Kennicutt, Jr., Steward Observatory, University of Arizona

Abstract

Local Group galaxies offer a unique opportunity to obtain information on the global structure of the interstellar medium, with sufficient spatial resolution to provide detailed diagnostics of the phase structure, physical conditions, and dynamics of the gas. This paper discusses recent observations of the ionized phases of the ISM in the spiral and irregular galaxies of the Local Group, and describes several recent applications to the problems of star formation and ISM dynamics.

1 Introduction

Most of what we know about the physics of the interstellar medium– its structure, phase balance, dynamics, and evolution— comes from observations of our own Galaxy. Consequently our theoretical understanding of the interstellar medium (ISM) is tuned to reproducing the properties of a localized region of roughly solar abundance and intermediate star formation rate in a single Sbc galaxy. Local Group (LG) galaxies offer a unique opportunity to extend the scope of this work to ISM in galactic environments spanning the full range of densities, pressures, abundances, star formation rates, and binding potential. They offer the optimal combination of accessible angular scale, which makes it possible to obtain global measurements of the ISM, with sufficient sensitivity and spatial resolution to provide quantitative diagnostics of the ISM structure, kinematics, and physical conditions. LG galaxies are also the optimum laboratories for studying the complex interactions between massive stars, supernovae, and the ISM, on scales ranging from single stars to giant complexes containing thousands of massive stars.

This paper describes recent observations of the ionized phases of the ISM in LG galaxies (see the companion article by Christine Wilson on the cold ISM). I will concentrate on optical emission line observations and X-ray surveys, where many important advances have been made in recent years. Along the way I will highlight several specific applications, including the stellar content, luminosity functions, and kinematics of star forming regions, star/ISM interactions, and the systematics of chemical abundances in the ISM. My goal is not to present a comprehensive review but rather to illustrate applications for which observations of LG galaxies are especially important.

2 The Magellanic Clouds

The Magellanic Clouds offer several unique advantages for studying the ISM in galaxies. Their distances are close enough to provide excellent spatial resolution (1" = 0.25–0.35 pc), yet distant enough that most interstellar structures such as H II regions and supernova remnants (SNRs) have angular sizes of several arcminutes or less. The galaxies also exhibit the full range of star forming regions, from individual protostellar clouds to giant H II regions like 30 Doradus, the largest star forming complex in the LG. Hence it is not surprising that the Clouds are the best studied objects (apart from the Galaxy) in the LG. I first summarize surveys of the ionized gas at visible, X-ray, and radio wavelengths, then briefly discuss recent studies of the stellar content and dynamics of star forming regions.

2.1 Emission-Line Surveys

Comprehensive catalogs of the H II regions in the Magellanic Clouds are available from the photographic surveys of Henize (1956) and Davies, Elliot, & Meaburn (1976). The only complete photometric catalog is that of Kennicutt & Hodge (1986), based on PDS scans of a set of calibrated Hα plates obtained

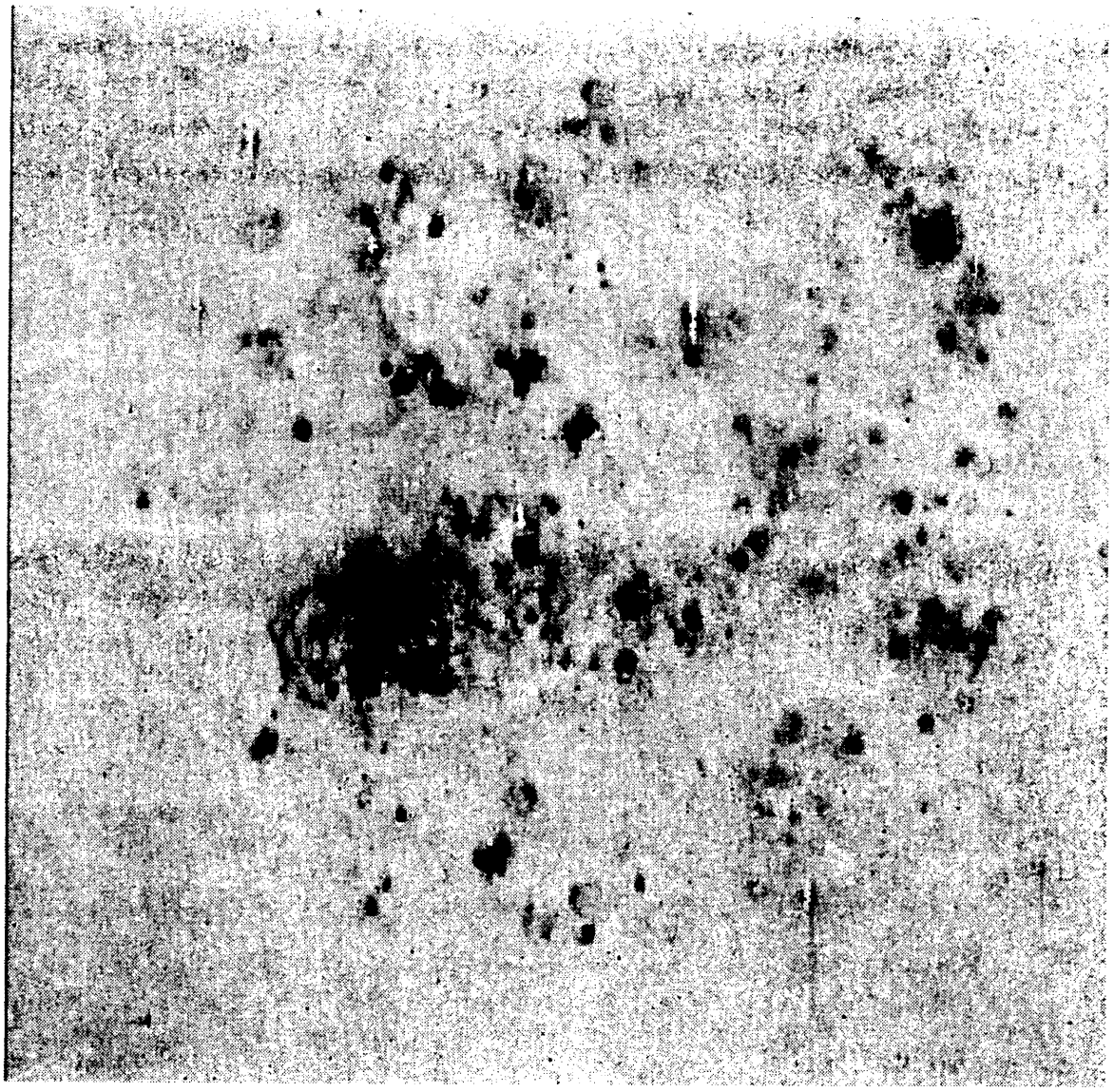

Figure 1: The LMC imaged in Hα with the LCO Parking Lot Camera, from Kennicutt *et al.* (1994).

with the Curtis Schmidt telescope at CTIO. Subsequently the plates were rescanned, and maps covering both galaxies at 5" resolution have been used for various applications (e.g., Ye, Turtle, & Kennicutt 1991; Chu *et al.* 1993; Caplan *et al.* 1994). The limited S/N, photometric accuracy, and dynamic range of the photographic maps restrict the range of applications for which they can be used, however.

The large angular sizes of the Clouds makes complete CCD imaging of the galaxies prohibitive, but progress is gradually being made. Le Coarer *et al.* (1993) have used an imaging Fabry-Perot spectrometer mounted on a 36 cm telescope to map the Hα emission in the SMC. Complete velocity cubes have been constructed with a resolution of 9" spatially and 16 km s^{-1} in velocity. The summed line images reach a limiting emission measure of 11 cm^{-6} pc, sufficient to detect most of the diffuse line emission.

Direct images in Hα have also been obtained for both the LMC and SMC using a TI CCD detector mounted behind an 85 mm camera lens, an updated version of the "Parking Lot Camera" (Bothun & Thompson 1988). These data have been processed and analyzed by Kennicutt *et al.* (1994), and Figure 1 shows the continuum-subtracted image of the LMC. The image scale is 36" per pixel, giving a total field of 8 deg. This is roughly how the LMC would appear in Hα if observed from outside the LG. The emission at bright levels is dominated by the large H II complexes, such as the 30 Doradus superassociation in the southeast and the N11 region in the northwest. Filamentary structures and

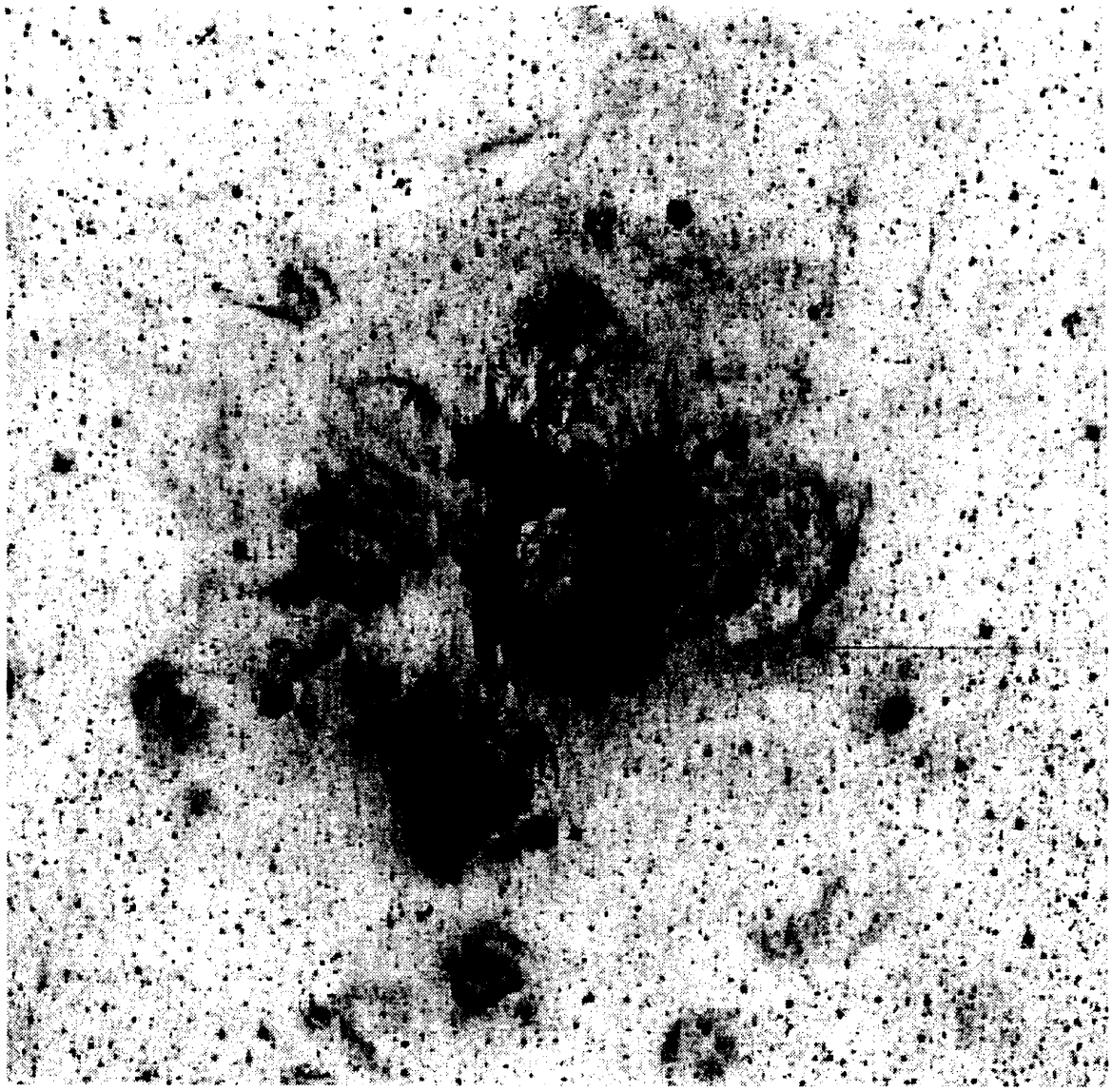

Figure 2: The region around the giant H II region N44 in the LMC, imaged in Hα with the Curtis Schmidt Telescope at CTIO by Chris Smith. Ten minute CCD exposure.

diffuse emission dominate the structure of the galaxy at fainter levels (cf. Meaburn 1980; Hunter 1994). These structures contribute 35–40% of the integrated Hα luminosity of the LMC and SMC (Kennicutt *et al.* 1994), and a considerably larger fraction of the ionized gas mass.

The installation of a large-format CCD camera on the Curtis Schmidt telescope at CTIO now makes it possible to contemplate a deep high resolution emission-line survey of the Clouds. As a proof of concept Chris Smith has obtained CCD images in Hα, [SII], and [OIII] for selected H II regions, SNRs, and supershells. Figure 2 shows an Hα image of the N44 region in the LMC, taken from this study. The image reveals a wealth of low surface brightness structure around the main H II region, that is barely if at all detectable in the previous photographic studies of Davies *et al.* (1976) and Kennicutt & Hodge (1986).

As an illustration of the importance of high S/N imagery of this kind, Figure 3 shows the same region as observed in a pointed *ROSAT* observation by Chu *et al.* (1993). The X-ray emission from the prominent central bubble in N44 is evident, but the map also shows X-ray emission associated with two faint optical shells to the northeast and west of the main nebula. As discussed by Chu *et al.* (1993) these are probably SNRs in the periphery of N44. Much of the X-ray emission in the Magellanic Clouds is associated with such faint extended optical nebulosity, with emission measures of order a

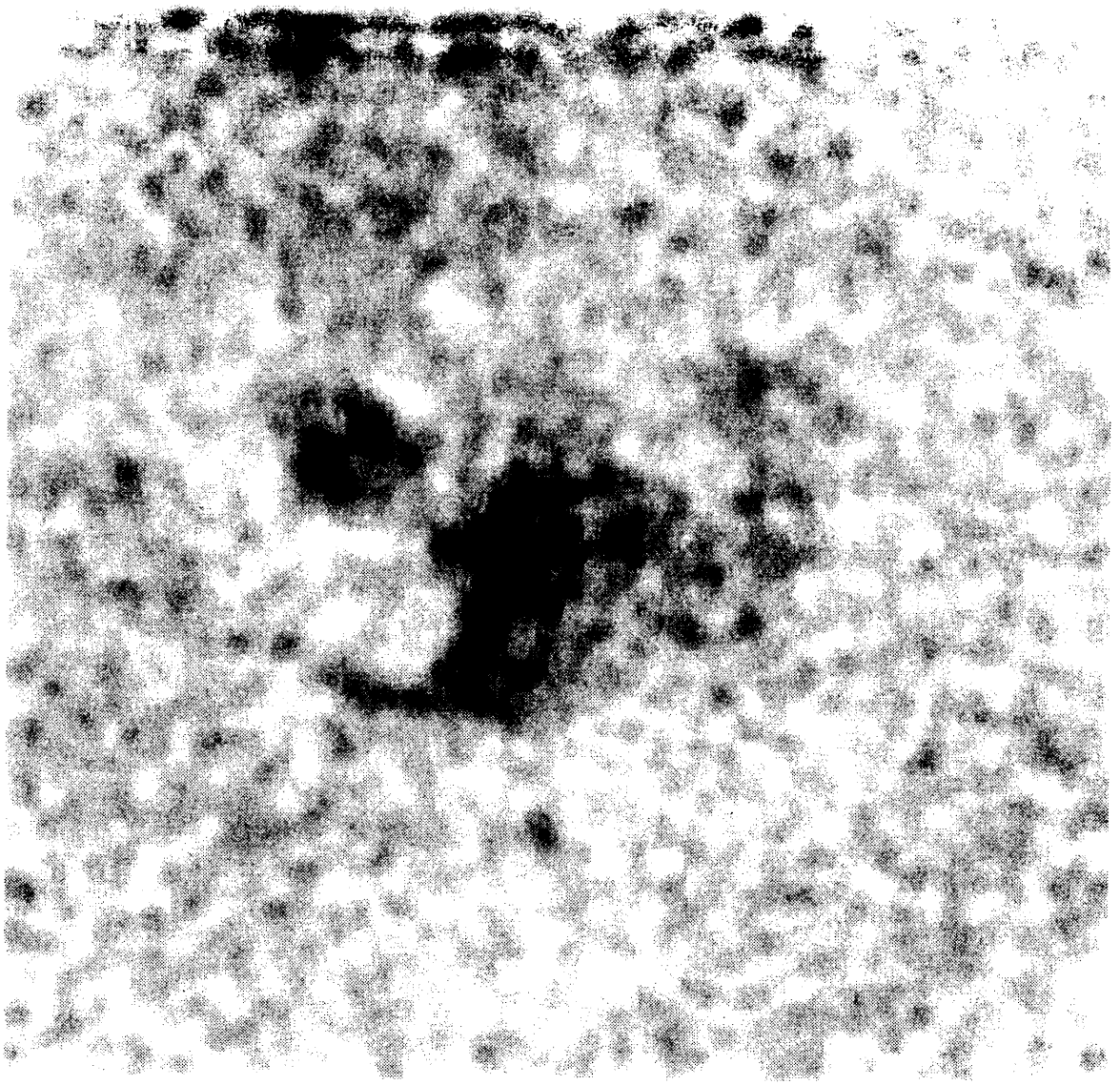

Figure 3: Smoothed *ROSAT* PSPC image of N44, covering the same field as shown in Hα in Figure 2.

few hundred cm^{-6} pc or less. This emphasizes the need for deep emission-line maps to constrain the physical conditions in the associated ionized shells.

With a 2048x2048 STIS chip it would be possible to map both the LMC and SMC in approximately 100 fields. Such a survey would provide an unprecedented database on the ionized ISM in a galaxy, and serve as a valuable resource for studying H II regions and SNRs, and for interpretation of the *ROSAT*, *IRAS*, and radio continuum observations. Such a survey is in the planning stages (C. Smith, private communication).

2.2 X-Ray and Radio Continuum Surveys

Extensive information on the hot ISM in the Clouds is available from the *Einstein* and *ROSAT* surveys. The first *Einstein* source searches identified numerous sources which were coincident with radio and/or optical SNRs (Long, Helfand, & Grabelsky 1981; Mathewson *et al.* 1983, 1985). Many of these were located in or near large OB/HII associations (Mathewson *et al.* 1983, 1985; Chu & Kennicutt 1988b). However these catalogs selected against extended diffuse sources which might be associated with evolved H II regions. Subsequent analysis of the *Einstein* IPC images at the positions of the cataloged OB associations revealed several extended X-ray sources, probably formed by SNRs erupting within the

shell nebulae (Chu & Mac Low 1990; Wang & Helfand 1991a, b).

The *ROSAT* survey has provided a wealth of information on the extended X-ray emission in the LMC and SMC. Preliminary studies of selected objects such as 30 Doradus, N44, N4D, and N9 in the LMC (e.g., see Fig. 3) have revealed previously undetected sources, most likely produced by SNRs (Chu *et al.* 1993, 1994; Smith *et al.* 1994). Moreover *ROSAT* clearly detects the large-scale diffuse X-ray emission from the LMC ISM, including emission from the large supershells (Bomans, Dennerl, & Kürster 1994). Some extended emission was marginally detected by *Einstein* (Wang *et al.* 1991), but *ROSAT* is at least an order of magnitude more sensitive, sufficient to carry out robust analyses of the physical conditions in this gas.

Radio continuum surveys of the Magellanic Clouds have been completed by Turtle's group at Sydney. The galaxies have been mapped at 843 MHz with the Molonglo Observatory Synthesis Telescope (e.g., Ye, Turtle & Kennicutt 1991). This resolution of the maps are approximately 43" × 46", and when combined with Hα maps or higher frequency radio maps these are especially effective for identifying SNRs. Selected regions have also been mapped at 1415 MHz with the Fleurs Synthesis Telescope. The completion of the Australia Telescope now makes it possible to map selected H II regions and SNRs with resolutions of several arcseconds. Dickel *et al.* (1994) have mapped the 30 Doradus region at 13 cm, with 7.5" resolution. This has made it possible to compare the radio and optical brightness on a point-by-point basis and measure the variation of extinction in the region.

2.3 Stellar Content and IMF of Giant H II Regions

The proximity of LG galaxies, especially the Magellanic Clouds, makes them indispensible for studying the resolved young stellar populations and IMF (see the reviews in this volume by Hodge and Greggio). Especially valuable are studies of the embedded OB stellar populations in H II regions, because studies of the integrated light of these regions are often used to test for systematic variations in the IMF. The LG H II regions offer an opportunity to look for IMF variations directly, and to test the nebular diagnostic methods which are applied in more distant galaxies.

Detailed studies of the stellar content of several OB/HII regions have been made by several investigators (e.g., Lee 1990; Massey *et al.* 1990a, b; Parker *et al.* 1992; Hill, Madore, & Freedman 1994). The most extensively studied region to date has been 30 Doradus. The inner 7′ of the nebula (~100 pc) contains ~2400 stars brighter than $V = 18$ (Parker & Garmany 1993), not including the compact core cluster around the central object R136. HST images show over 200 stars within the inner $R = 3.3$" = 0.8 pc (Campbell *et al.* 1992; Malumuth & Heap 1994). At a distance of 10 Mpc these two regions would correspond to angular scales of 2" and 0.017", respectively! Clearly one can only resolve these regions for Local Group, even with HST.

A color-magnitude diagram of 30 Dor, based on photometry of 1230 stars and classification spectra for 140 blue stars is shown in Figure 4 (Parker & Garmany 1993). This is illustrative of the quality of data that can be obtained for the Magellanic Cloud OB/HII associations. Overlaid are evolutionary tracks, which can be used to derive the mass function. Parker & Garmany (1993) derive an IMF slope $\Gamma \equiv d(logN)/d(logm) = -1.5 \pm 0.2$, and Malumuth & Heap (1994) find evidence for a significantly shallower slope in the inner core of the H II region. It is interesting to note that previous measurements of the IMF slope in 30 Dor, based on *UBV* photometry alone, range from $\Gamma = -0.8$ to -2.0 for the same region! This emphasizes the need for complete observations supplemented by spectroscopy for these regions before any conclusions about the form or variation of the upper IMF can be drawn.

2.4 ISM Kinematics and Dynamics

Mechanical energy input from stellar winds and supernovae dominate the energetics of the ISM, and the LMC and SMC offer the opportunity to observe these processes over a wide range of physical and temporal scales. The most important diagnostics of these star/ISM interactions are the X-ray emission, discussed earlier, and the kinematics of the ionized gas. Kinematic surveys of H II regions in the Magellanic Clouds by Smith & Weedman (1970, 1971, 1972) and Meaburn (1981, 1984, 1988) revealed that these regions are characterized by supersonic 'turbulent' motions superimposed on discrete structures the 1–100 pc scale.

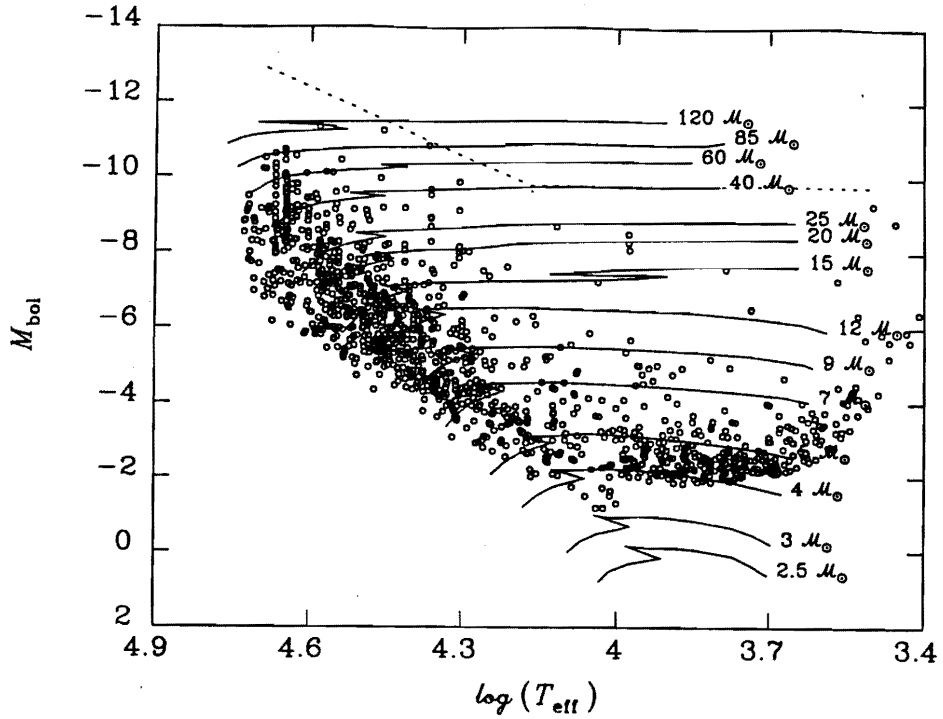

Figure 4: H-R diagram for the central 7′ region of 30 Doradus, from Parker & Garmany (1993).

By combining observations of the nebular velocity field with X-ray and optical emission-line diagnostics of the ionized gas it is possible to trace the transfer of energy into the ISM on scales ranging from individual wind-blown bubbles and SNRs to galactic-scale supershells. Such a systematic study is being carried out by Chu and her collaborators, using high-resolution echelle spectra obtained at CTIO and ROSAT X-ray observations. Velocity fields have been measured for a large sample of SNRs (Chu & Kennicutt 1988a, b), and diverse sample of LMC/SMC H II regions, including 30 Doradus (Chu *et al.* 1992, 1993; Chu & Kennicutt 1994a, b). IUE absorption line spectra are also being used to obtain additional information on the ionization structure and kinematics of the region (Chu *et al.* 1994).

An example of what can be learned from such data is shown in Figure 5, which shows the velocity structure of Hα in the inner $9' \times 9'$ core of 30 Doradus. This simulated multi-slit spectrum was generated from 37 separate long-slit echellograms. The velocity range in each spectrum is ± 300 km s^{-1}. The velocity field exhibits a complexity which mirrors the chaotic filamentary morphology of the nebula. Several distinct types of velocity structures can be identified, a smooth supersonic turbulent background field, slow expanding shells most likely associated with wind-driven flows, and fast expanding shells, with velocities of over ± 100 km s^{-1} and diameters of 1–30 pc (Meaburn 1984). Most of the latter are associated with extended X-ray sources, and are probably produced by SNRs erupting inside 30 Dor (Chu & Kennicutt 1994). The largest expanding networks require input energies which exceed even those of single supernovae; most likely these are true supershells produced by the combined effects of supernovae and stellar winds from entire OB associations. The results strongly hint that the cataloged SNRs in the Clouds represent only a fraction of the total population; a comparable number may be 'hidden' in the large OB/HII complexes, and are either masked by the bright foreground nebulosity, or lie hidden in the low density wind-driven shell nebulae (Chu & Mac Low 1990).

The complete coverage of the echelle data allow us to derive the global energetics of the 30 Doradus region, and compare the relative amounts of kinetic energy contained in the different types of structures. The total kinetic energy, $\sim 10^{52.2}$ ergs in the central 9′, exceeds by at least an order of magnitude the gravitational binding energy of the H II region. This implies that 30 Doradus is in the process of blowing itself apart. When one considers the total wind and supernova energy available in the entire

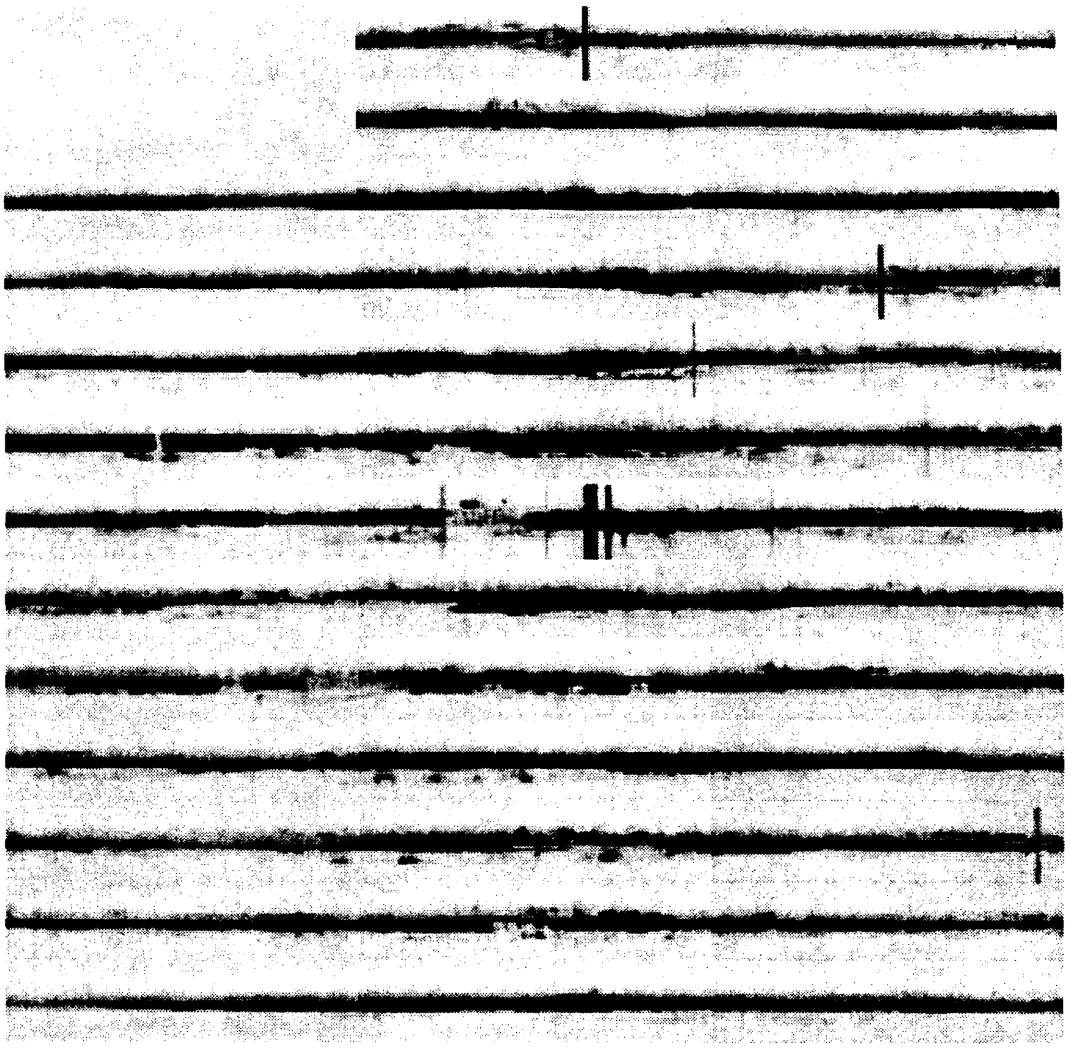

Figure 5: Echelle mosaic showing velocity structure of the Hα emission line in the central $9' \times 9'$ core of 30 Doradus. Velocity scale for each spectrum is ± 300 km s^{-1}. The continuum source near the center is R136.

30 Dor superassociation, it is likely that the complex will evolve into a complex comparable in size to the largest LMC supershells over the next 10–30 Myr. By extending this work to a larger range of OB/HII associations it should be possible eventually to trace the evolution of such structures over the full range of age and scales (cf. Oey, this conference).

3 M31 and M33

The Sb galaxy M31 offers a marked contrast in ionized ISM properties from most of the other spiral and irregular galaxies in the LG. It is a relatively gas-poor galaxy, with most of the atomic and molecular gas concentrated in a ring which is coincident with the main spiral arms. High resolution HI maps show a highly resolved structure dominated by HI 'holes' (Brinks & Shane 1984). The most complete Hα survey of M31 is the photographic study of Pellet *et al.* (1978). The H II regions follow the same ring distribution as the cold gas. Photographic photometry of the brighter H II regions was published by Kennicutt, Edgar, & Hodge (1989), and deep CCD photometry of the NE ring has been published by Walterbos & Braun (1992, 1994). This has been analyzed in conjunction with a deep radio continuum survey (Braun 1990) to study the SNR population (Braun & Walterbos 1993; also see the paper by Prins in this volume). A wide-field CCD image of the entire galaxy has also been obtained recently by

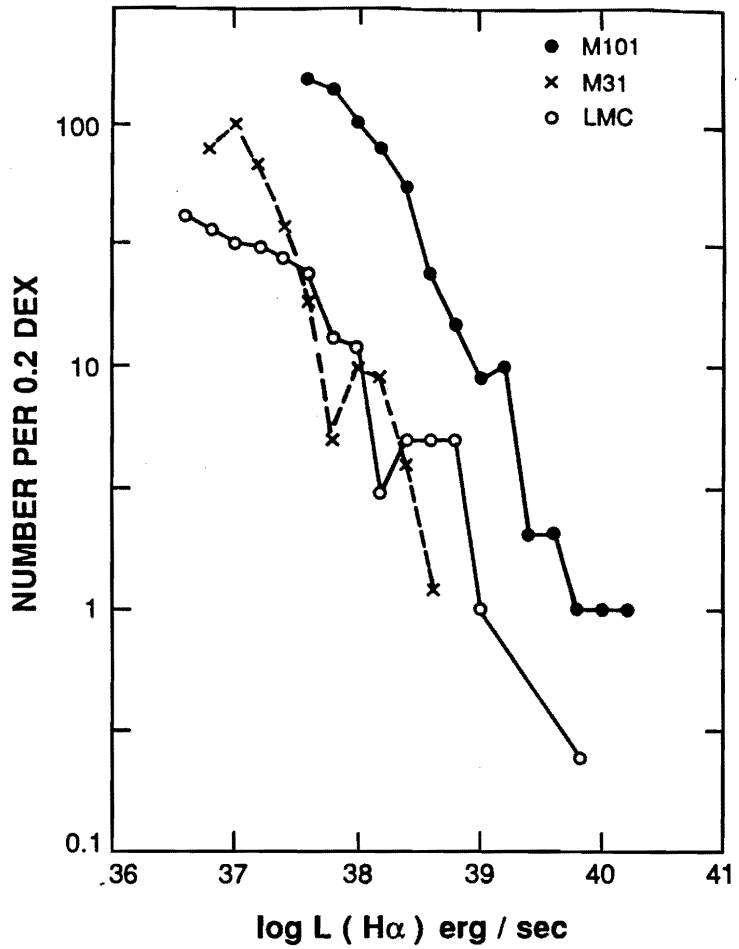

Figure 6: Hα differential luminosity functions for H II regions in M31, LMC, and M101, from Kennicutt *et al.* (1989).

Devereux (private communication).

The most striking difference immediately apparent in M31 is the faintness of the H II region population. This is demonstrated quantitatively in Figure 6, which compares the H II region luminosity function (LF) in M31 with those for the LMC and the Sc galaxy M101 (Kennicutt *et al.* 1989). The comparison of M31 with the LMC is especially instructive, as both galaxies are well resolved and the LFs should be relatively free of incompleteness problems. Even though M31 contains far larger number of H II regions than the LMC, reflecting its much larger mass, the LMC has at least 10 H II regions that are brighter than any region in M31. Analysis of a larger galaxy sample shows that the differences between M31 and the LMC and M101 reflect a general trend along the Hubble sequence, with earlier galaxies containing smaller numbers of H II regions per unit galaxy mass or luminosity, and a steeper LF slope (Kennicutt *et al.* 1989). The magnitude of the trend is strong; for galaxies of comparable mass the luminosity of the brightest H II region increases by nearly an order of magnitude between each successive Hubble type. The physical origin of the change is unclear, it may reflect underlying changes in the mass spectra of atomic/molecular clouds, or it may be due in part to changes in star formation efficiency and/or the IMF.

Deep CCD imagery of M31 shows that 40% of the line emission is produced by diffuse ionized gas (DIG; Walterbos & Braun 1994). Such DIG is observed in our own Galaxy and in many edge-on galaxies; M31 provides an excellent opportunity to study the physical conditions and ionization mechanisms for this gas in a nearby, well-resolved system. The most complete study to date is based on an Hα and [SII] imaging survey by Walterbos & Braun (1992, 1994). The average [SII]/Hα ratio in

the DIG is 0.5, increasing to 0.7–1 in the faintest regions. This is comparable to the values observed in other galaxies, and consistent with photoionization in a dilute radiation field or shock ionization. The deprojected surface brightness and inferred scale height of the DIG is lower than many of the best studied edge-on galaxies, a result which the authors attribute to the relatively low star formation rate in M31.

M31 also offers a rare opportunity to study the ionized gas in a spiral bulge. Extended emission in Hα + [NII], [SII], and [OII] was discovered by Jacoby, Ford, & Ciardullo (1985), and a detailed analysis of the structure, kinematics, and excitation of this gas has been published by Ciardullo *et al.* (1988). The gas appears to be flattened in a disk, but with an orientation which is different from the inner stellar disk, and with a pronounced asymmetry or warp. Filaments of emission extend over a region of ~500 pc. The [SII] doublet ratio shows a strong gradient over the inner arcminute of the galaxy, indicating a drop in electron density from of order $\geq 10^4$ to 10^2 over radii of 0–200 pc. The properties of this ISM are consistent with its having originated from stellar mass loss in the bulge, probably under the influence of a galactic wind in the bulge (Ciardullo *et al.* 1988).

The LG Sc galaxy M33 has also been the subject of surveys in Hα (Courtès *et al.* 1987), the radio continuum (Viallefond *et al.* 1986), and X-rays (Trinchieri, Fabbiano, & Peres 1988). Several groups have obtained deep CCD Hα images of the galaxy, but little is published yet. The galaxy shows a bright DIG over most of the disk, which exhibits an extensive filamentary structure not unlike that observed in the LMC (e.g., Courtès *et al.* 1987; Hester, private communication). The atomic gas in M33 shows similar structure with large HI holes and filaments (Deul & van der Hulst 1987). Considerable analysis of the physical properties of specific objects such as the H II regions (e.g., Viallefond & Goss 1986; Oey & Massey 1994) and SNRs (e.g., Long *et al.* 1990; Duric *et al.* 1993; Smith *et al.* 1993) has been published, but relatively little quantitative analysis of the large-scale properties of the ISM in this galaxy is available.

4 Dwarf Irregular Galaxies

The dwarf irregular galaxies in the LG provide valuable information on the ISM structure, star formation, and chemical evolution in systems that span a hundredfold range in luminosity. Deep Hα CCD imaging has revealed ionized gas in at least a dozen LG or near-LG dwarfs, including (in decreasing order of luminosity from $M_B \simeq$ -16 to -11): IC 10, NGC 6822, Sextans A and B, IC 1613, IC 5152, WLM, UGC-A86, Leo A, GR8, DDO 210, and the Sagitarious DIG (Hodge *et al.* 1988, 1989b, 1990, 1994; Hodge & Lee 1990; Strobel *et al.* 1991; Hodge, private communication). It is notable that most if not all of the gas-rich dwarfs in the LG have some detectable level of current star formation.

The galaxies show a wide diversity in both the global levels of star formation (see the review by Hodge in this volume) and in the morphologies of the star forming regions. The H II regions tend to have lower surface brightness and more extended stucture than those found in more massive spirals (Kennicutt 1984), but it is not clear whether this is due to physical differences in the ISM environments, differences in the properties of the embedded stellar populations, or merely a selection effect caused by the small populations sizes in the dwarf galaxies. Recently Collier, Hodge, & Kennicutt (1994) performed a multivariate analysis of the H II regions in NGC 6822, a particularly well studied dwarf, in an effort to identify physical correlations with the nebular structure and morphology. No systematic trends were identified. It is interesting that similar H II region morphologies— low surface brightness regions, a preponderance of ring or shell regions— are often observed in the outer disks of spirals such as M33, in regions where the ambient gas densities and metallicities are more similar to those in the dwarfs. It would be interesting to perform a similar statistical test to see whether these apparent radial trends in spirals are significant, and are consistent with the observed properties of the H II regions in dwarf galaxies.

The relatively low surface densities of H II regions in some of the dwarfs also makes it possible to obtain a complete unbiased inventory to very faint levels, without the problems of crowding and extinction that often plague searches for faint H II regions in spirals. Hodge, Lee, & Kennicutt (1989a) exploited this fact to measure the luminosity function (LF) of the H II regions in NGC 6822 to a completeness limit below L(Hα) = 10^{35} ergs s^{-1}. The transition between the low-luminosity regime,

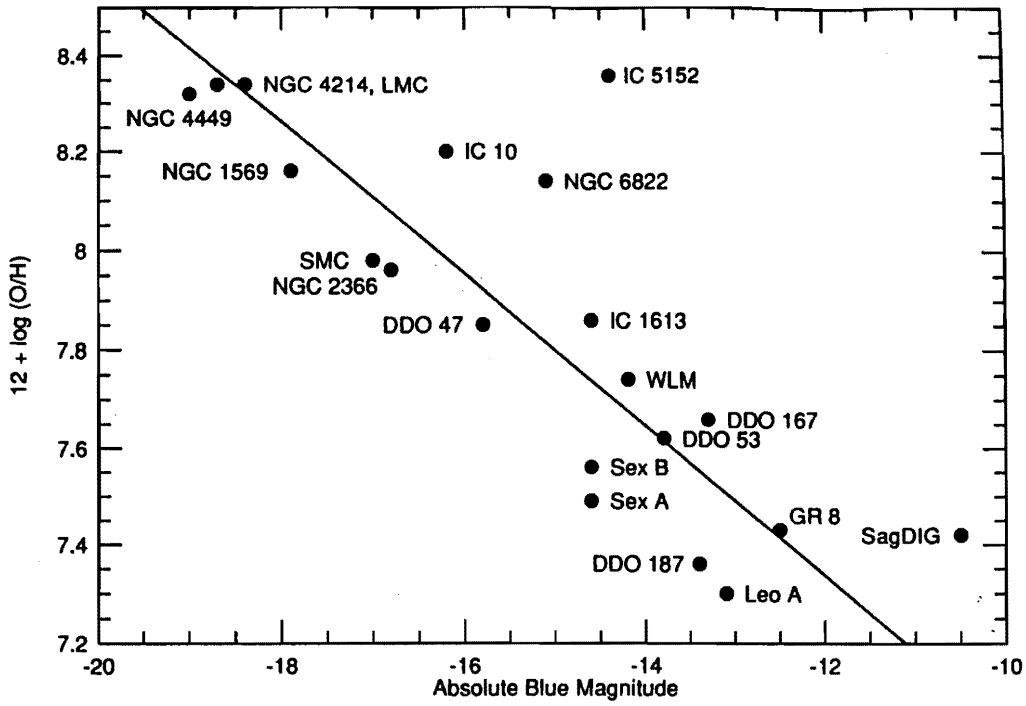

Figure 7: Correlation between H II region oxygen abundance and absolute magnitude for irregular galaxies, from Skillman *et al.* (1989).

where the LF shape is dominated by the stellar UV luminosity function, and an upper power-law which traces the luminosity function of OB associations is clearly seen.

Perhaps the most valuable application of these observations is for studying the chemical abundances and evolution in primitive galactic environments. Most of what we know about chemical evolution at low abundances has been based on studies of dwarf emission-line galaxies such as I Zw 18 or II Zw 40, but the techniques used to identify these galaxies nearly assures that their chemical properties will be polluted by the current bursts of star formation. The LG dwarfs, on the other hand, represent systems of similar mass, luminosity, and gas content in normal, relatively quiescent phases of evolution, and as such they offer pristine chemical environments for studying the composition of low-mass galaxies, and for constraining the primordial helium abundance.

Abundance surveys of LG dwarf irregulars have been carried out by Skillman, Terlevich, & Melnick (1989), and Skillman, Kennicutt, & Hodge (1989). Figure 7, taken from the latter paper, shows the relation between oxygen abundance and absolute magnitude for the LG dwarfs along with several other nearby irregular galaxies. The data confirm the existence of a well defined abundance-luminosity relation, suggested earlier by Lequeux *et al.* (1979) and Talent (1980). Subsequent measurements of spirals show that this relation extends to spirals, and is nearly coincident with the well-known metallicity-luminosity relation in spheroidal galaxies (Garnett & Shields 1987; Zaritsky, Kennicutt, & Huchra 1994). The most metal-poor LG dwarf measured so far, GR8, has an oxygen abundance of roughly 1/30 solar (Skillman, Terlevich, & Melnick 1989), approaching I Zw 18, the most metal-poor Pop I galaxy known. This offers ample illustration of how problems as global as cosmological nucleosynthesis can be constrained by observations of the LG.

I am grateful to the many colleagues who loaned slides or viewgraphs, or provided papers in advance of publication: You-Hua Chu, Robin Ciardullo, Nick Devereux, Jeff Hester, Deidre Hunter, Paul Hodge, Greg Shields, Chris Smith, and Rene Walterbos. My research was supported by the National Science Foundation through grant AST90-19150.

References

Bomans, D.J., Dennerl, K., & Kürster, M.; 1994, A&A, in press.

Bothun, G.D., & Thompson, I.B.; 1988, AJ, **96**, 877.

Braun, R.; 1990, ApJS, **72**, 761.

Braun, R., & Walterbos, R.A.M.; 1993, A&AS, **98**, 327.

Brinks, E., & Shane, W.W.; 1984, A&AS, **55**, 179.

Campbell, B. et al.; 1992, AJ, **104**, 1721.

Caplan, J., Ye, T., Deharveng, L., Turtle, A.J., & Kennicutt, R.C.; 1994, A&A, submitted.

Chu, Y.-H., & Kennicutt, R.C.; 1988a, AJ, **95**, 1111.

Chu, Y.-H., & Kennicutt, R.C.; 1988b, AJ, **96**, 1874.

Chu, Y.-H., & Kennicutt, R.C.; 1994, ApJ, in press.

Chu, Y.-H., Kennicutt, R.C., Schommer, R.A., & Laff, J.; 1992, AJ, **103**, 1545.

Chu, Y.-H., & Mac Low, M.-M.; 1990, ApJ, **365**, 510.

Chu, Y.-H., Mac Low, M.-M., Garcia-Segura, G., Wakker, B., & Kennicutt, R.C.; 1993, ApJ, **414**, 213.

Chu, Y.-H., Wakker, B., Mac Low, M.-M., & Garcia-Segura, G.; 1994, AJ, submitted.

Ciardullo, R., Rubin, V.C., Jacoby, G.H., Ford, H.C., & Ford, W.K.; 1988, AJ, **95**, 438.

Collier, J., Hodge, P., & Kennicutt, R.C. 1994; PASP, submitted.

Courtès, G., Petit, H., Sivan, J.P., Dodonov, S., & Petit, M.; 1987, A&A, **174**, 28.

Davies, R.D., Elliot, K.H., & Meaburn, J.; 1976, MemRAS, **81**, 89.

Deul, E.R., & van der Hulst, J.M.; 1987, A&AS, **67**, 509.

Dickel, J.R., Milne, D.K., Kennicutt, R.C., Chu, Y.-H., & Schommer, R.A.; 1994, AJ, **107**, 1067.

Duric, N., Viallefond, F., Goss, W.M., & van der Hulst, J.M.; 1993, A&AS, **99**, 217.

Garnett, D.R., & Shields, G.A.; 1987, ApJ, **317**, 82.

Henize, K.G.; 1956, ApJS, **2**, 315.

Hill, R.J., Madore, B.F., & Freedman, W.L.; 1994, ApJ, in press.

Hodge, P., Kennicutt, R.C., & Lee, M.G.; 1988, PASP, **100**, 935.

Hodge, P., Kennicutt, R.C., & Strobel, N.; 1994, PASP, submitted.

Hodge. P., & Lee, M.G.; 1990, PASP, **102**, 41.

Hodge, P., Lee, M.G., & Gurwell, M.; 1990, PASP, **102**, 849.

Hodge, P., Lee, M.G., & Kennicutt, R.C.; 1989a, PASP, **101**, 32.

Hodge, P., Lee, M.G., & Kennicutt, R.C.; 1989b, PASP, **101**, 640.

Hunter, D.A.; 1994, AJ, **107**, 565.

Jacoby, G.H., Ford, H., & Ciardullo, R.; 1985, ApJ, **290**, 136.

Kennicutt, R.C.; 1984, ApJ, **287**, 116.

Kennicutt, R.C., Edgar, B.K., & Hodge, P.W.; 1989, ApJ, **337**, 761.

Kennicutt, R.C., & Hodge, P.W.; 1986, ApJ, **306**, 130.

Kennicutt, R.C., Bresolin, F., Bomans, D., & Bothun, G.; 1994, in preparation.

Le Coarer, E., Rosado, M., Georgelin, Y., Viale, A., & Goldes, G.; 1993, A&A, **280**, 365

Lee, M.G.; 1990, Ph.D. thesis, University of Washington.

Lequeux, J., Peimbert, M., Rayo, J.F., Serrano, A., & Torres-Peimbert, S.; 1979, A&A, **80**, 155.

Long, K.S., Blair, W.P., Kirshner, R.P., & Winkler, P.F.; 1990, ApJS, **72**, 61.

Long, K.S., Helfand, D.J., & Grabelsky, D.A.; 1981, ApJ, **248**, 925.

Malumuth, E.M., & Heap, S.R.; 1994, AJ, **107**, 1054.

Massey, P., Garmany, C.D., Silkey, M., & DeGioia-Eastwood, K.; 1989, AJ, **97**, 107.

Massey, P., Parker, J.W., & Garmany, C.D.; 1990, AJ, **98**, 1305.

Mathewson, D.S., Ford, V.L., Dopita, M.A., Tuohy, I.R., Long, K.S., & Helfand, D.J.; 1983, ApJS, **51**, 345.

Mathewson, D.S., Ford, V.L., Tuohy, I.R., Mills, B.Y., Turtle, A.J., & Helfand, D.J.; 1985, ApJS, **58**, 197.

Meaburn, J.; 1980, MNRAS, **192**, 365.

Meaburn, J.; 1981, MNRAS, **196**, 19P.

Meaburn, J.; 1984, MNRAS, **211**, 521.

Meaburn, J.; 1988, MNRAS, **235**, 375.

Oey, M.S., & Massey, P.; 1994, ApJ, in press.

Parker, J.W., Garmany, C.D., Massey, P., & Walborn, N.R.; 1992, AJ, **103**, 1205.

Parker, J.W., & Garmany, C.D.; 1993, AJ, **106**, 1471.

Pellet, A., Astier, N., Viale, A., Courtès, G., Maucherat, A., Monnet, G., & Simien, F.; 1978, A&AS, **31**, 439.

Skillman, E.D., Kennicutt, R.C., & Hodge, P.W.; 1989, ApJ, **347**, 875.

Skillman, E.D., Melnick, J., Terlevich, R., & Moles, M.; 1988, A&A, **196**, 31.

Smith, M.G., & Weedman, D.W.; 1970, ApJ, **161**, 33.

Smith, M.G., & Weedman, D.W.; 1971, ApJ, **169**, 271.

Smith, M.G., & Weedman, D.W.; 1972, ApJ, **172**, 307.

Smith, R.C., Chu, Y.-H., Mac Low, M.-M., & Oey, M.S.; 1994, preprint.

Smith, R.C., Kirshner, R.P, Blair, W.P., Long, K.S, & Winkler, P.F.; 1993, ApJ, **407**, 564.

Strobel, N.V., Hodge, P., & Kennicutt, R.C.; 1991, ApJ, **383**, 148.

Talent, D.L.; 1980, Ph.D. thesis, Rice University.

Trinchieri, G., Fabbiano, G., & Peres, G.; 1988, ApJ, **325**, 531.

Viallefond, F., & Goss, W.M.; 1986, A&A, **154**, 357.

Viallefond, F., Goss, W.M., van der Hulst, J.M., & Crane, P.C.; 1986, A&AS, **64**, 237.

Walterbos, R.A.M., & Braun, R.; 1992, A&AS, **92**, 625.

Walterbos, R.A.M., & Braun, R.; 1994, ApJ, in press.

Wang, Q., Hamilton, T., Helfand, D.J., & Wu, X.; 1991, ApJ, **374**, 445.

Wang, Q., & Helfand, D.J.; 1991a, ApJ, **370**, 541.

Wang, Q., & Helfand, D.J.; 1991b, ApJ, **373**, 497.

Ye, T., Turtle, A.J., & Kennicutt, R.C.; 1991, MNRAS, **249**, 772.

Zaritsky, D., Kennicutt, R.C., & Huchra, J.P.; 1994, ApJ, **420**, 87.